



The sand deposit underneath the Ishtar Temple in Assur, Iraq: Origin and implications for the foundation of the goddess's cult and sanctuary

Mark Altaweel ^{a,*}, Andrea Squitieri ^b , Eileen Eckmeier ^c, Eduardo Garzanti ^d, Karen Radner ^e

^a Institute of Archaeology, University College London, 31-34 Gordon Square, London WC1H 0PY, United Kingdom

^b Department of Cultural Heritage: Archaeology and History of Art, Cinema and Music, University of Padova, Piazza Capitaniato 7, 35139 Padova, Italy

^c Institute for Ecosystem Research, Kiel University, Olshausenstraße 75, 24118 Kiel, Germany

^d Department of Earth and Environmental Sciences, University of Milano-Bicocca, Piazza della Scienza 4, 20126 Milan, Italy

^e History Department, Ludwig Maximilian University of Munich (LMU), Geschwister-Scholl-Platz 1, 80539 Munich, Germany

ARTICLE INFO

Keywords:

Mesopotamia
Assur
Early Bronze Age
Temple foundation
Sand deposit
Mineralogy
Upper Fars
Goddess Ishtar
Goddess Shawushka (Shaushka)

ABSTRACT

This study presents the first-ever systematic mineralogical investigation of sands from an archaeological context in Iraq, establishing a methodological precedent for future geoarchaeological investigations in Mesopotamia and studies of ancient architecture more broadly. The sand derives from a deposit underneath the Ishtar Temple at Assur (Ashur; modern Qal'at Sherqat) on the Tigris River, once the political and religious centre of the Assyrian state. Since the earliest layers of the main Assur Temple are inaccessible, this sanctuary is the oldest temple explored through excavation at the site. Thus, data from its early strata are critical for understanding the city's earliest history. In 2024, coring within the temple cella by the Assur Excavation Project revealed a thick sand layer beneath its foundations, deliberately placed before construction. As no comparable deposits exist locally, the material was sourced explicitly for this purpose. Sand foundations for monumental buildings are known from southern Mesopotamia but are here attested for the first time in the north. Mineralogical analyses indicate that the Ishtar Temple sands mostly consist of epidote-group minerals associated with glaucophane, zoisite, lawsonite sourced from blueschist-facies metamorphic rocks. Their provenance is plausibly from nearby aeolian sand recycled from the Injana Formation and ultimately traceable to the Zagros Mountains, linked to Assur via the Lesser Zab River. Thus, while southern building traditions were adopted, the sand was not imported from the south but sourced in the region and ultimately derived from the eastern Zagros Mountains. Radiocarbon dating from the floor above the sand yielded a date range of 2896–2702 calBC (95.4 % probability), providing new information for the debate surrounding the temple's foundation and its role within Mesopotamian cultural history. These results significantly inform debates on the origins of Ishtar's cult at Assur.

1. Introduction

The archaeological site of Assur (also Ashur; modern Qal'at Sherqat, 35.45 N, 43.26 E) lies in northern Iraq, on the western bank of the Tigris River, some 100 km downstream from Mosul, close to the modern city of al-Sherqat (also al-Shirqat) and its important river crossing (Fig. 1). Assur, which sits on a mostly Miocene limestone ridge, was the capital city of the Assyrian state and as such used from the 3rd millennium BCE to the late 7th century BCE, when that state collapsed. The site remained continuously occupied until the first centuries of the common era, as the most recent excavations have revealed (Radner and Squitieri, 2024; 2025). By the early 2nd millennium BCE, Assur had developed into a

major urban centre featuring monumental temples and palaces (Andrae, 1938).

Walter Andrae first excavated Assur between 1903 and 1914, during which he uncovered most of the city's monumental buildings located in the Inner Town, including the Isthmar Temple, which is the subject of the present study (Andrae, 1922; 1935). Subsequent archaeological investigations at Assur were conducted by the Iraqi State Board of Antiquities and Heritage (SBAH) and several German research teams from the 1980s to the early 2000s, with several lengthy interruptions (Miglus, 2003). In April 2022, SBAH granted permission to Ludwig Maximilian University of Munich (LMU) and Münster University to conduct new research and excavations at Assur.

* Corresponding author.

E-mail addresses: m.altaweel@ucl.ac.uk (M. Altaweel), andrea.squitieri@unipd.it (A. Squitieri), eeckmeier@ecology.uni-kiel.de (E. Eckmeier), eduardo.garzanti@unimib.it (E. Garzanti), k.radner@lmu.de (K. Radner).

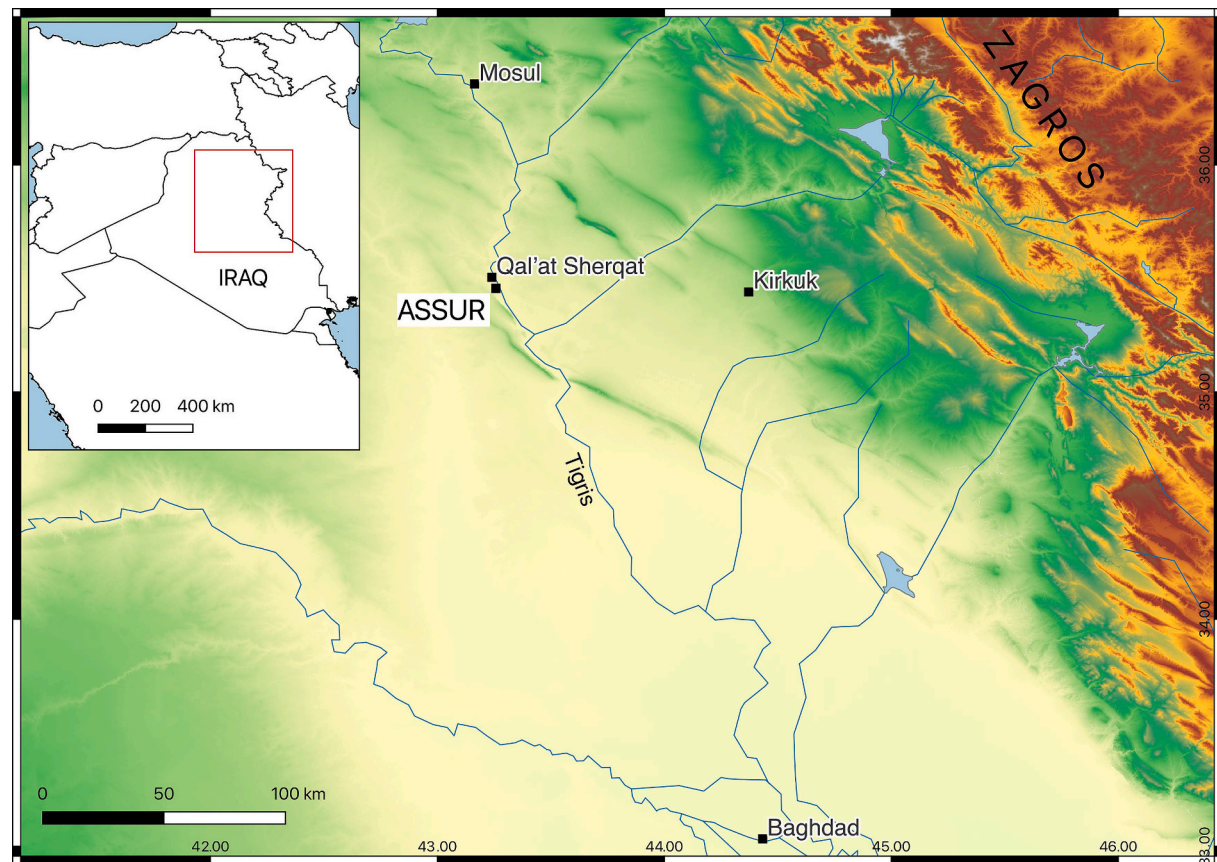


Fig. 1. The location of Assur (35.45 N, 43.26 E) in northern Iraq.

Whereas the Assur Excavation Project's excavation work since 2023 has focused on the New Town area of Assur (Radner and Squitieri, 2024; 2025), the research programmes in geophysics and geoarchaeology cover the entire site. In February 2024 and during a short follow-up season in February 2025, we used coring to investigate the foundation of the Ishtar Temple, whose original cella level had been exposed by Andrae. Unlike other areas he had excavated, these remains have remained easily accessible due to their shallow position beneath the modern surface. We aimed to reach the temple's earliest level with the corer and determine the depth of the natural ground, while hoping to expose samples suitable for radiocarbon dating. When we took the first core in 2024, we were surprised to uncover a thick deposit of sand underneath the Ishtar Temple's earliest building phase (Altaweel 2025). These sands had not been reported in previous publications, indicating that Andrae's investigations had not reached the deposit and that he was unaware of its existence (Andrae, 1922; 1035), a fact that all later studies reflect (see Bär, 2003a; Schmitt, 2012; Beuger, 2013). Additionally, the recovery of small charcoal fragments and ashes from within the deposit allowed its absolute dating by means of radiocarbon analysis at the Curt-Engelhorn-Zentrum Archäometrie of the Reiss-Museen in Mannheim (Germany), thus providing the first-ever absolute date from the Ishtar Temple and at the same time the oldest absolute date so far recorded for Assur. Moreover, it establishes a *post quem* date for the foundation of this important sanctuary.

This paper presents the results of mineralogical research and constitutes the first application of such analysis to a culturally significant architectural context in the study of ancient Mesopotamia. After providing background information about the city of Assur and the Ishtar Temple, we discuss the analytical methods used to assess the origin of geological data, specifically as applied to sands and comparable materials. We then lay out the methodology used in this study, followed by a presentation of the results of our analyses. This leads firstly to a

discussion of the origin of the analysed sands and secondly to an evaluation of the historical and archaeological implications.

2. Background

2.1. The ancient city of Assur in northern Mesopotamia

The Ishtar Temple of Assur was first exposed by Walter Andrae (Andrae, 1922; 1935). More recently, the results of his excavations were reevaluated by Bär (2003a; older phases), Schmitt (2012; younger phases), and Beuger (2013; ceramic finds). The temple forms part of a building complex dedicated to the goddess Ishtar and later the god Nabû, where Andrae (1938) documented a sequence of superimposed structures attributed to the period from the mid-3rd to the mid-1st millennia BCE (Fig. 2).

In his investigations, Andrae uncovered some walls that he assigned to the temple's earliest phase, designated as "Temple H," which was thought to have been built directly on the virgin soil (Andrae, 1938: 72; Bär, 2003a: 36). While Andrae dated Temple H to the beginning of the 3rd millennium BCE in the Early Dynastic I (c. 2900–2700 BCE; Andrae, 1938: 72) based on material culture and stylistic evidence, later scholarship reassigned it to the Early Dynastic III period of the archaeological chronological classification of southern Mesopotamia (e.g. Bär, 2003a: 38; Meinhold, 2009: 17–18), conventionally dated to around 2600–2340 BCE. As Temple H corresponds to the earliest occupation level ever identified at Assur, this chronological assessment implies that the site's earliest known settlement occurred in the Early Dynastic III period.

Apart from the chronological uncertainties surrounding the foundation of the Ishtar Temple, another key issue concerns the origins of the cult of the goddess Ishtar at Assur (Andrae 1938: 72). The style and iconography of the several statuary items found by Andrae within the temple's third millennium BCE phases (mainly from phases G and F,



Fig. 2. The Ishtar/Nabû temple complex (white dashed line) in the Inner Town of Assur, and the location of the four sediment cores discussed in this paper.

which followed phase H stratigraphically, see Bär, 2003b: table 2; also Meinhold, 2009: 18–21) have led scholars to link the Ishtar cult at Assur to southern Mesopotamia, where she was then worshipped under the Sumerian name of Inana (also Inanna). Others, however, have rejected this view and prefer to see the cult of Ishtar at Assur as having a more local origin; this discussion was conveniently summarised by Jürgen Bär (2003b: 144). In northern Mesopotamia and the surrounding mountain regions, a similar deity was worshipped under the Hurrian name Šawuška (or Šauška; see Wegner, 1981; Seidl, 2005). At nearby Nineveh (modern Mosul), where Ishtar is the most prominent deity, she is identified with the Hurrian goddess (Haas, 1979; Schwemer, 2001: 460–461, 464; Meinhold, 2009: 169), and this is also the case at Arbela (modern Erbil; see Seidl, 2005: 169; MacGinnis, 2014).

The results of the present study affect both the dating of the Ishtar Temple's oldest building phase and, consequently, the oldest occupation at Assur. In addition, they provide entirely new data elucidating aspects of the question concerning the origins of the Ishtar cult at Assur.

2.2. Recent mineralogical analyses in archaeology

In recent years, studies of sediments, including sands or specific aggregates, in archaeological contexts have received growing attention, but they have been more focused on the Mediterranean world rather than Mesopotamia. Studies have revealed not only the geological origins of archaeological sediments but have also shed light on technological and other cultural patterns in antiquity. For example, mineralogical characterisations of Roman and Byzantine mortars in the Mediterranean have traced the sources of quartz, feldspar, and volcanic temper used, demonstrating how craft specialists selected aggregates to optimise strength and durability (e.g., Secco et al., 2019). Similarly, analyses of glass-making sands have highlighted differences between Egyptian, Levantine, and Western Mediterranean deposits, contributing to debates

on trade and resource utilisation for glass (e.g., Brems et al., 2015). Beyond elucidating construction and craft production, sedimentary mineral assemblages from archaeological contexts can potentially inform on site formation processes and environmental dynamics. Our work in Iraq is pioneering in this regard, as it is the first systematic mineralogical study of sands conducted on a temple's foundation and settlement stratigraphy. This approach helps establish a vital baseline for future research by demonstrating how sand deposits help to address a site's foundation as well as its cultural landscape.

3. Methodology

3.1. Coring for sediment recovery

Sediments were sampled during on-site fieldwork in February 2024 using a Cobra Pro TT percussion corer (Fig. 3). Four core samples, registered as C21–C24, were taken from inside the temple's cella, with cores reaching about 2 m below the surface. Their locations were selected in areas corresponding to the remains of the earliest temple phase (Temple H), identified based on Andrae's plans, which were georeferenced using the later temple's structures still visible on the surface today (Fig. 4).

Three window-sampling cores (C21–C23) were taken, allowing sediments to be collected directly through the tube opening of the corer. A fourth core (C24) was obtained using a sequence of two clear plastic tubes and exported in its entirety from Iraq for laboratory analysis in Europe in June 2024.

3.2. Description of core sediment and analyses of samples

Core C24, which was taken near cores C21–C22 in a sequence of two clear plastic tubes, was labelled C24-1 and C24-2 (Fig. 7). The total of



Fig. 3. Coring at the Ishtar Temple in Assur using the Cobra Pro TT corer for sediment column recovery. The modern street level is indicated.

200 cm of core material was visually inspected, and 23 sediment layers and textures were identified (Table 2) based on their visible features and stratigraphy. From all stratigraphical layers, subsamples were taken to analyse the particle sizes of the material on fractions $<2000\text{ }\mu\text{m}$, after the aggregates had been carefully crushed and the material $>2000\text{ }\mu\text{m}$ was removed by sieving. Grain size distribution was analysed by laser diffraction spectrometry on a Mastersizer 3000 particle size analyser (Malvern Instruments). The texture size classes correspond to international standards as described by the WRB (2022) (clay $<2\text{ }\mu\text{m}$, silt 2–63 μm , sand 63–2000 μm). Before the measurement, samples were treated with 35 % hydrogen peroxide to destroy organic matter, with 0.5 M sodium acetate buffer solution to remove carbonate, and then with sodium pyrophosphate to prevent particle coagulation. Colours have been determined using a spectrophotometer (Konica Minolta CM-700d) on sediment material. The obtained spectral information was converted to the CIE (L^* , a^* , b^*) (CIE 1976) and Munsell colour systems, utilising SpectraMagic NX software (Konica Minolta).

High-resolution heavy-mineral analyses were conducted at the University of Milano-Bicocca on sand samples 36 and 37 taken from the complete core C24. Heavy minerals were separated by centrifugation in sodium polytungstate (density $\sim 2.90\text{ g/cm}^3$) and recovered by partial freezing with liquid nitrogen. On grain mounts, 200 transparent heavy-

mineral (tHM) grains were point-counted at suitable regular spacing under the petrographic microscope by Marta Barbarano. All grains of uncertain identification were checked with Raman spectroscopy (Andò and Garzanti, 2014).

The volume percentage of total and transparent heavy minerals relative to total sediment is expressed as the heavy mineral concentration (HMC) and transparent HMC (tHMC) indices (Garzanti and Andò, 2019). The zircon, tourmaline, and rutile (ZTR) index is the sum of zircon, tourmaline, and rutile over total transparent heavy minerals and is used to estimate the durability of the assemblage (Garzanti, 2017). Heavy mineral data are summarised below; the complete data are provided in the *Supplemental Materials* (Table HM).

4. Results

4.1. Descriptions of the cores taken from within the Ishtar Temple at Assur

Fig. 5 presents the lithological succession drawings of cores C21, C22, and C23, which were taken with the window sampler. These visuals and the following descriptions of the three cores reflect observations made in the field during the extraction rather than the results of laboratory analysis.

In all three cores, the top layer (0–25 + cm) consisted of clay fill; small pieces of white calcite stones and ash were observed in places. These are fill materials and debris that had fallen into Andrae's earlier excavation trench within the Ishtar Temple, where the cores are located. Below this, the sediments remained clayey, using Folk's (1981) classification, and were relatively devoid of cultural materials, reflecting likely compacted material that had filled in.

In cores C22 and C23, at 73–80 cm and 95–100 cm below the surface, respectively, a gravel level was evident, mixed with some larger stones and pottery that reflects a likely floor level for Temple H (i.e., the earliest temple phase). Below this gravel layer, we found sandy, yellowish remains without pottery or other human-made materials except for the occasional small piece of charcoal. In C23, silty/clay material with possible mud brick debris was observed at 100–135 cm, but without the presence of pottery or pebbles. In the material from 135–150 cm, ash and charcoal were mixed with pottery: this appears to have been another, earlier floor level that included compacted cultural material.

From this lower floor level, an ash sample taken at a depth of 139 cm below the surface was exported in May 2025 and sent for radiocarbon analysis to the Curt-Engelhorn-Zentrum Archäometrie of the Reiss-Museen in Mannheim (Germany). This yielded the date range 2896–2702 calBC (95.4 % probability; Fig. 6 and Table 1), which fits within the Early Dynastic I.

In C21, between 70 and 190 cm, we observed an all-sand yellow layer with a few small pieces of charcoal. Around 190 cm, the sand layer ended, and very clayey sediments mixed with calcite granules started, without any cultural material. This clay layer continued to around 235 cm. The sediments below consist of rocks, and we stopped coring at around 250 cm as we had likely reached bedrock.

For C22, yellow sand material was observed from 100 to 190 cm. Around 165 cm, there were some pebbles and calcium nodules mixed with the sand. No cultural material was found in the sand layer. From a depth of around 190–200 cm, the corer encountered rocks again, hitting the level of the natural bedrock.

Core C23 shows that underneath the floor from which the radiocarbon sample was taken, the yellow sand layer was observed at a depth of 150–180 cm, without any cultural material but with some gypsum. From 180 cm onwards, pebbly material started, and we stopped coring, assuming that this was the top of the hard rocks of the natural bedrock.

The sediment in core C24, as shown in Tables 2 and 3 and Fig. 8, demonstrates a clear dominance of the sand fraction, with coarser grain sizes increasing toward the lower parts of the cores. A clear boundary at a depth of 77 cm indicates the transition between presumably younger sediment input into the room and the coarser material below. Above, the



Fig. 4. The locations of cores C21-C24 in the Ishtar Temple. The plan on the right, georeferenced from Andrae (1922: pl. 4), shows the oldest temple phase (Temple H) in red. After Altawee (2025: fig. B2.5).

sediments are divided into distinct layers of infillings, which include artefacts, e.g., pottery sherds at a depth of 40 cm. The sediment contains more silt, which is comparable to the current material on top of the site. A layer of rounded gravel at 51–54 cm depth and a distinctive layer of dark red and grey angular rock grit at 66–77 cm might have been part of an artificial surface or material that collapsed onto the floor. The red rock material was not identified as part of the local geology. Below 77 cm and up to about 125 cm depth is a transition area with mixed material containing rounded gravel and grit. Tiny charcoal particles have been detected up to a depth of 120 cm, although they might not be in situ. Below 125 cm, gypsum-rich material dominates in variable amounts and ratios, with clearly developed gypsum crystals. Gypsum is an important component of the prevailing bedrock material, along with marl.

4.2. Mineralogical analysis of sand

The sand analysed by the University of Milano-Bicocca consists of samples 36 and 37 from C24. These two samples originate from the top and bottom of the sand layer, around 100 cm and 200 cm below the surface, respectively.

The poor tHM suite of the two studied samples (tHMC 0.7) mainly consists of epidote-group minerals (51 % of total tHM; mainly Fe-epidote with common clinozoisite and rare zoisite) with subordinate amphibole (8–17 % tHM; blue-green to brown hornblende, actinolite, tremolite, and glaucophane), garnet (8–14 % tHM), apatite (3–11 % tHM), clinopyroxene (2–8 % tHM), titanite (4–5 % tHM), and minor tourmaline

(2–3 % tHM), anatase (1–3 % tHM), Cr-spinel (2 % tHM), zircon, rutile, and rare lawsonite, chloritoid, and andalusite. Most distinctive is the presence of minerals derived from blueschist-facies metamorphic rocks (i.e., glaucophane, zoisite, lawsonite). The invariable presence of celestite is noteworthy, representing as much as 9 % of sample 36 and 1 % of sample 37. Celestite is an authigenic mineral commonly found in sediments across hyperarid Arabia and is inferred to be related to the extensive circulation of evaporite brines. In southern Arabia, these brines are likely derived from dissolution and remobilisation of Pre cambrian salt (Angiolini et al. 2003).

4.3. The provenance of the sand deposit below the Ishtar Temple at Assur

The origin of the samples from the sand deposit below the Ishtar Temple at Assur can be evaluated by comparison with mineralogical data from other Mesopotamian fluvial and aeolian sands (Table 4).

Fig. 9 provides an image of the heavy minerals identified under the light microscope. As a preliminary observation, the tHM assemblage of the Assur sand samples does not match any fluvial sand in the region. The Assur sand samples are characterised by a notably poorer heavy-mineral assemblage, by a higher percentage of epidote, apatite and titanite, and by a lower percentage of amphibole and pyroxene relative to sand carried by the larger rivers in the region ($tHMC \geq 4$ in sand of the Tigris mainstream and of its Greater Zab and Lesser Zab tributaries; Fig. 10). The Lesser Zab sand is more similar but still richer in heavy minerals (tHMC 3.2), richer in amphibole and clinopyroxene, and with a lower epidote percentage. A greater similarity is observed with the

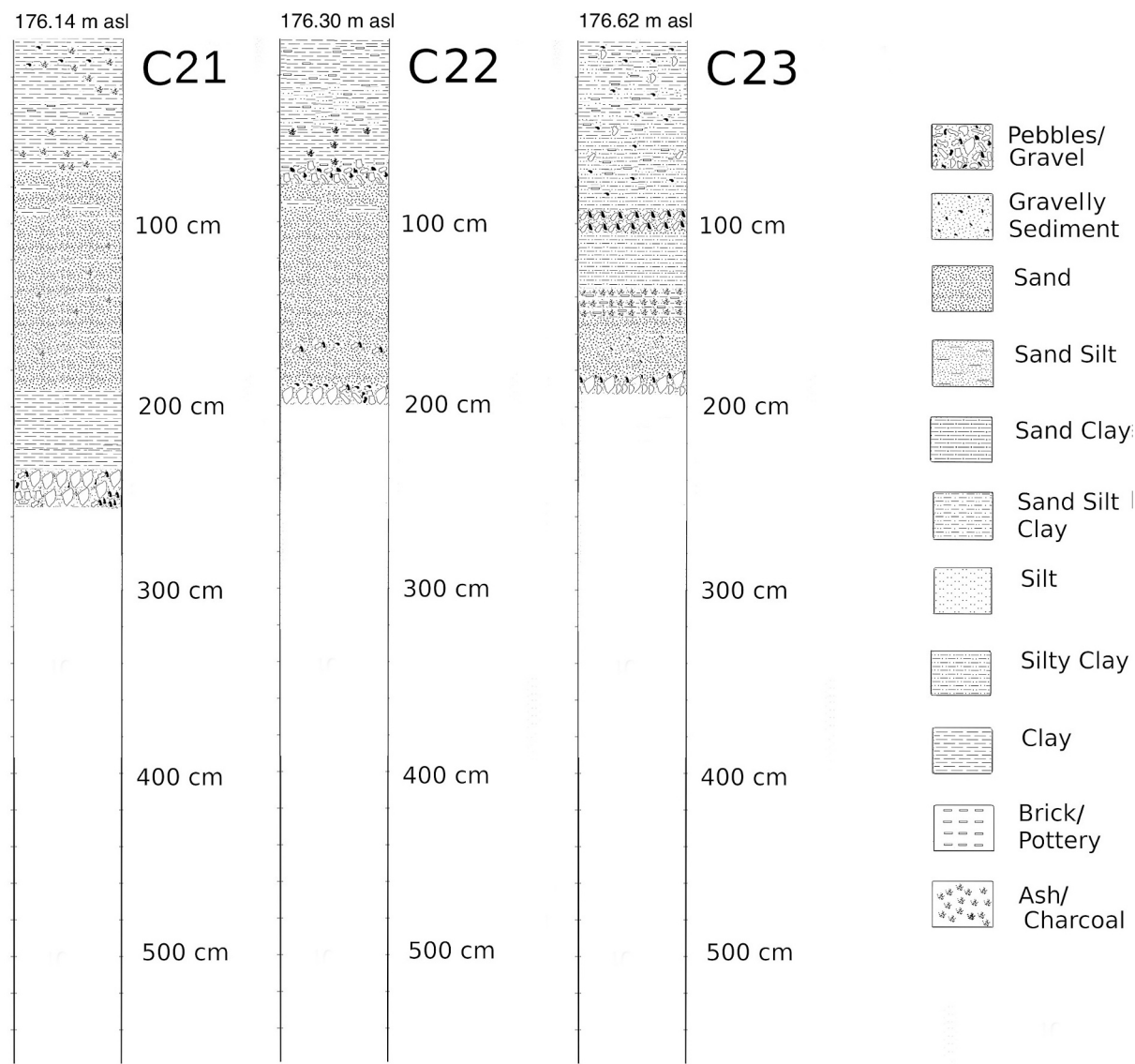


Fig. 5. Core drawings, with textual descriptions in the main text, from the three window samplers (C21-C23).

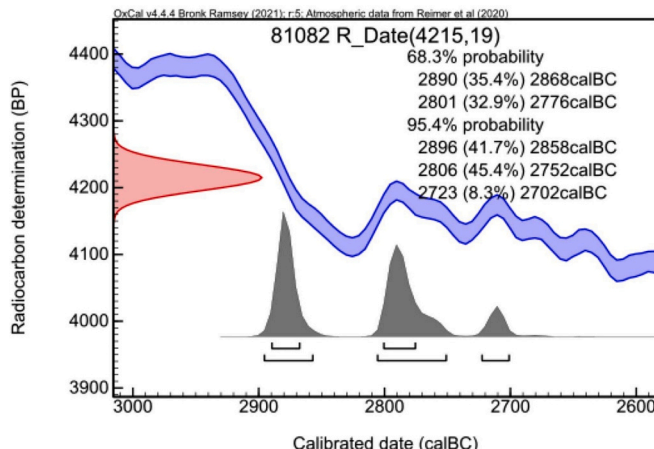


Fig. 6. Radiocarbon determination of an ash sample taken from core C23 at a depth of 139 cm. Analysis conducted at the Curt-Engelhorn-Zentrum Archäometrie (CEZA) of the Reiss-Engelhorn-Museen in Mannheim. Radiocarbon ages were calibrated using OxCal v4.4.4 (Bronk Ramsey 2021) and the IntCal20 atmospheric calibration curve (Reimer et al. 2020). Probability distributions (68.3 % and 95.4 %) were calculated using the standard Bayesian calibration algorithm implemented in OxCal.

Table 1

Summary table of the radiocarbon age determination (4215 ± 19 BP) for sample 81082.

Sample ID	Radiocarbon age (BP)	Software / calibration curve	Probability level	Calibrated age ranges (cal BC)
81,082	4215 ± 19	OxCal v4.4.4 (IntCal20)	68.30 %	2890–2868 (35.4 %); 2801–2776 (32.9 %)
81,082	4215 ± 19	OxCal v4.4.4 (IntCal20)	95.40 %	2896–2858 (41.7 %); 2806–2752 (45.4 %); 2723–2702 (8.3 %)

tHMC suite of aeolian dunes in the Baji area, 45 km to the SSE of Assur, which is moderately rich (tHMC 2.6) and contains higher amounts of epidote.

A similarity is also observed with upper Neogene sandstones of the Injana Formation exposed in the distant Najaf area, which contain a poor to moderately poor suite (tHMC 1.0), even richer in epidote. In a nearby region 160 km to the southeast, the Injana Formation is reported to contain a poor suite (average tHMC 0.8) containing zircon, tourmaline, rutile, garnet, apatite, hornblende, actinolite, tremolite-actinolite,

Table 2

Description of visible colour, texture, and characteristics of the sediments of core C24.

Layer/Nr	Depth cm	Description
C24-1-1	0–5	dark brown to reddish, dense, no artefacts
C24-1-2	5–8	dark brown with fine black layers, charcoal, organic fragments
C24-1-3	8–21	dark brown to reddish, dense, no artefacts
C24-1-4	21–28	dark brown to grey, secondary carbonates/gypsum, no artefacts
C24-1-5	28–40	dark brown to reddish, dense, secondary carbonates/gypsum, charcoal
C24-1-6	40–41	pottery fragments
C24-1-7	41–43	dark brown to grey, secondary carbonates/gypsum, charcoal
C24-1-8	43–51	dark brown to grey and reddish layers, secondary carbonates/gypsum, charcoal
C24-1-9	51–54	mainly gravel (rounded), no artefacts
C24-1-10	54–66	dark brown to reddish, dense, less secondary carbonates/gypsum, charcoal
C24-1-11	66–77	stone layer (abrupt start) with dark red and grey rock grit, secondary carbonates, charcoal
C24-1-12	77–92	light brown to reddish, few dark spots, dense, secondary carbonates/gypsum
C24-1-13	92–100	light brown to reddish, coarse light material, stones, secondary carbonates/gypsum
C24-2-14	100–103	dark brown, black gravel, grit, sand, charcoal
C24-2-15a	103–116	light brown to reddish, grit, very lose, gypsum
C24-2-15b	116–125	light brown to reddish, coarse light material, grit, very lose, gypsum, charcoal
C24-2-16	125–132	brown to reddish, partly very lose when gypsum, partly silt
C24-2-17	132–147	light brown to reddish, grit, very lose, gypsum
C24-2-18	147–156	grey grit, sand, layers of grey and red deteriorated rock (marl)
C24-2-19	156–162	reddish, very sandy, gypsum crystals
C24-2-20	162–169	grey grit (marl), sand, red loamy layers
C24-2-21	169–170	gypsum fragments
C24-2-22	170–181	grey and reddish, sand, grit, few larger rock fragments (marl)
C24-2-23	181–200	brownish-reddish, grit, few larger rock fragments (marl)

glaucophane, diopside, aegirine, epidote, zoisite, titanite, Cr-spinel, and opaques (mainly magnetite; [Kettanah and Abdulrahman, 2022](#)).

Most revealing is the presence, in Injana sandstones and in the Lesser Zab sand as well as in the Assur sand samples, of minerals indicative of provenance from high-pressure, low-temperature mafic metamorphic rocks (glaucophane, zoisite, lawsonite), thus testifying to provenance from blueschist-facies rocks exposed in the Zagros orogen ([Talbot, 2019](#)). The peculiar presence of celestite, also found in abundance in test pits along Najaf Sea paleo-shorelines ([Briant et al., 2024](#)), indicates the reworking of local sulfate crusts.

The Assur sand samples 36 and 37 are unlikely to represent fluvial sand from the Tigris River or from any of its major tributaries in the region. Mineralogical similarities with the Lesser Zab sand draining the Zagros suture ([Garzanti et al., 2016](#)) and especially with the sandstones of the upper Neogene Injana Formation and with local dune fields

indicate aeolian reworking of sand possibly shed by the Injana Formation and ultimately derived from the Zagros suture belt, including blueschist-facies metamorphic rocks, as shown by the principal component analysis ([Fig. 11](#)). The common presence of celestite, presumably reworked from a sulfate crust precipitated from sulfate-saturated waters in Iraq's dry climate, reinforces this hypothesis. [Fig. 12](#) and [Fig. 13](#) show the Raman spectra that helped identify celestite and lawsonite present in the samples.

5. Discussion

Our investigations have revealed the presence of a thick layer of sand at the foundation level of the first Ishtar Temple of Assur, which did not contain any visible artefacts or other materials besides the sediment. The radiocarbon dating of charcoal material from the walking surface

Table 3

Analytical data of the sediments (texture and colour values) in core C24.

Layer/Nr	Depth	Clay	Silt	Sand	Munsell	Munsell	Munsell	L*	a*	b*
	cm	%	%	%	Hue	Value	Chroma			
C24-1-1	0–5	4	47	48	9.6 YR	5.2	2.6	53.7	4.8	16.0
C24-1-2	5–8	5	55	40	0.1 Y	4.5	2.1	46.0	3.7	13.4
C24-1-3	8–21	3	38	59	9.4 YR	4.6	2.5	47.6	5.1	15.4
C24-1-4	21–28	3	32	65	1.4 Y	5.3	1.9	55.0	2.1	12.7
C24-1-5	28–40	5	50	45	9.2 YR	4.6	2.5	46.9	5.2	14.9
C24-1-6	40–41	n.d.	n.d.	n.d.	n.d.	n.d.	n.d.	n.d.	n.d.	n.d.
C24-1-7	41–43	3	35	62	2.0 Y	5.4	1.7	55.8	1.4	11.8
C24-1-8	43–51	3	36	61	9.7 YR	5.3	2.4	54.8	4.2	14.8
C24-1-9	51–54	1	16	83	9.4 YR	5.2	2.9	53.6	5.6	18.0
C24-1-10	54–66	3	40	57	9.2 YR	5.4	2.8	55.4	5.5	17.3
C24-1-11	66–77	2	22	76	5.7 YR	4.5	1.8	46.6	6.0	8.8
C24-1-12	77–92	0	11	89	9.0 YR	6.2	3.4	63.2	6.3	20.4
C24-1-13	92–100	0	15	85	9.7 YR	6.3	3.0	64.3	4.8	18.6
C24-2-14	100–103	2	20	78	9.7 YR	5.5	2.4	56.6	4.2	15.1
C24-2-15a	103–116	2	15	83	9.2 YR	5.4	2.8	55.8	5.4	16.9
C24-2-15b	116–125	1	23	76	9.4 YR	5.8	2.6	59.3	4.7	16.0
C24-2-16	125–132	2	23	75	9.3 YR	5.5	2.9	56.3	5.6	17.7
C24-2-17	132–147	3	25	72	9.2 YR	5.3	2.7	54.4	5.4	16.6
C24-2-18	147–156	3	26	71	2.0 Y	6.3	2.2	64.5	1.4	15.1
C24-2-19	156–162	3	18	79	9.2 YR	5.4	2.5	55.9	4.9	15.4
C24-2-20	162–169	4	20	76	0.3 Y	6.0	2.6	61.7	3.7	16.9
C24-2-21	169–170	3	19	78	9.8 YR	5.2	2.5	53.8	4.4	15.9
C24-2-22	170–181	11	28	60	0.3 Y	4.9	2.1	50.6	3.4	13.5
C24-2-23	181–200	4	20	76	9.8 YR	5.9	2.8	61.1	4.6	17.7

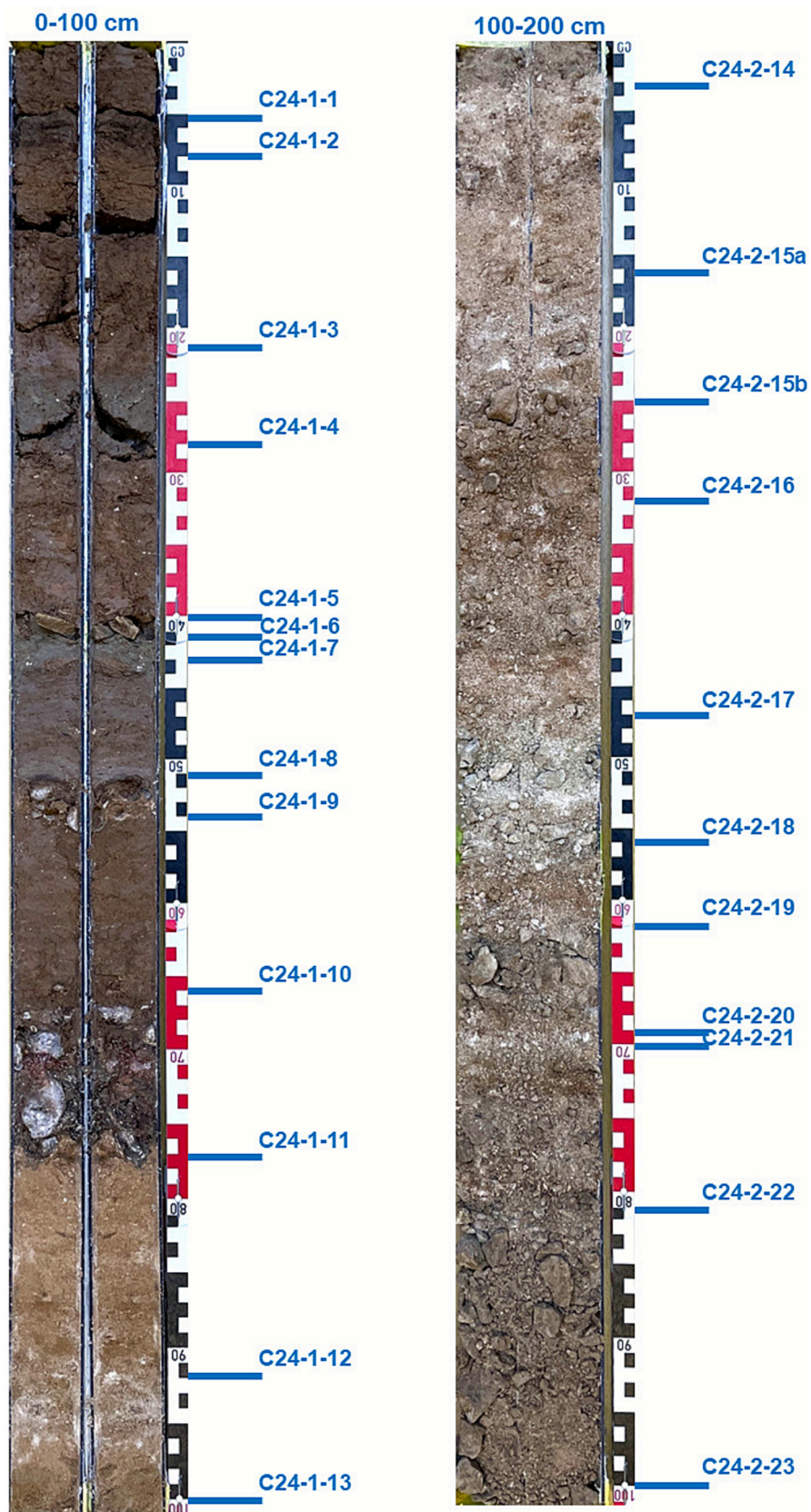


Fig. 7. Cores C24-1 (0–100 cm depth) and C24-2 (100–200 cm depth).

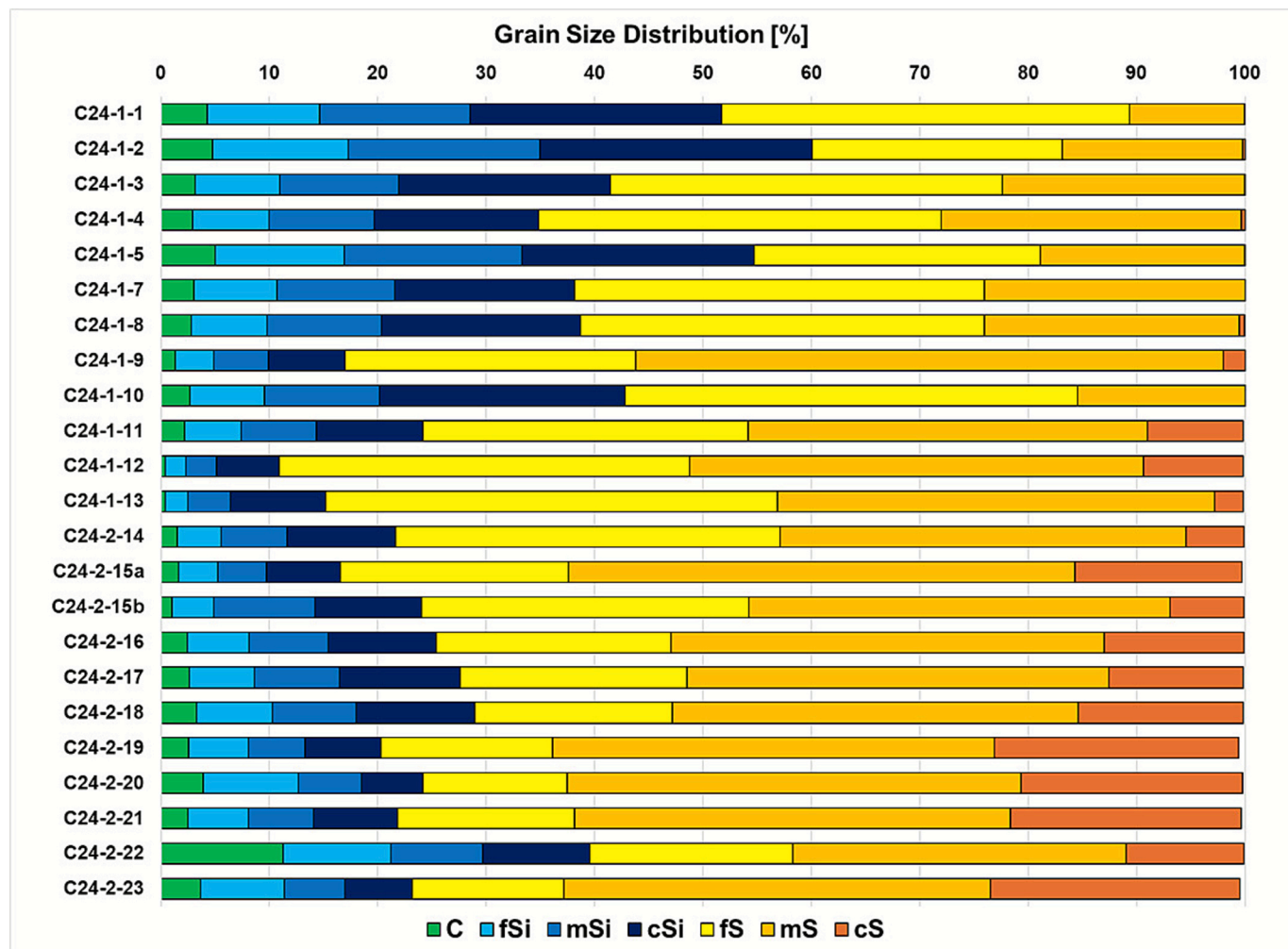


Fig. 8. Grain size distribution of the sediments assigned to the specific layers in C24. Layer 6 consisted only of ceramics and was not analysed (C = clay; Si = silt; S = sand; f = fine; m = medium; c = coarse).



Fig. 9. Microscopic image showing identified heavy minerals from sand in sample 36 from core C24, with all present transparent heavy mineral species labelled.

directly above the sand deposit resulted in a date range of 2896–2702 calBC (95.4 % probability). This considerably predates the conventional dating of the Ishtar Temple's first building phase to the Early Dynastic Period III (ca. 2600–2340 BCE) and is more in line with the excavator Walter Andrae's dating of the earliest temple structure to the beginning of the third millennium BCE. Since the oldest known occupation layers of Assur were reached at the Ishtar Temple, this new radiocarbon date range also alters our understanding of the timeline for the settlement of Assur.

In ancient Mesopotamian culture, preparing temple foundations was a crucial step in construction, as these needed to be ritually purified to serve as a dwelling for the deity (Ambos, 2004; Averbeck, 2010). In southern Mesopotamia, this purification was typically achieved by laying down clean sand at the base of the temple (Ellis, 1968: 132–33; Leacroft and Leacroft, 1974). However, the data presented in this study are the first to document such a practice in northern Mesopotamia, where the site of Assur is located.

Importantly, laying a purified sand deposit is not a feature in the construction of all temples in Assur. In February 2025, further coring was undertaken in some of the other temples exposed by Andrae, including the Sin-Shamash and Anu-Adad temple complexes (Werner, 2009; 2016). We encountered no indication of sand deposits underneath their foundations. Already in spring 2024, we had attempted to core in the cella of the Assur Temple, but the height of the deposited layers, including those dating to modern times, proved to be very deep, and it was impossible to reach the foundation (Altawee, 2025). Nevertheless, the results from coring in the other temple complexes indicate that the case of the Ishtar Temple was different from some of the other important shrines at Assur. This suggests that the presence of a sand deposit in its foundation is culturally significant.

The geological characteristics at the site of Assur are dominated by

the Injana (Late Miocene) and the Fatha (Middle Miocene) formations, with the Fatha Formation stretching in a northwest-southeast direction south of the modern city of al-Sherqat, and along the Tigris River. It also forms the anticlinal limestone hills west of the archaeological site of Assur. The Fatha Formation is characterised by cycles of green marl, limestone and gypsum, whereas the Injana Formation consists of clay and sandstone layers (Sissakian et al., 2014).

Our analysis of the sand samples from the Ishtar Temple suggests a likely regional origin for these materials; we believe the materials were ultimately sourced from the Zagros Mountains, using aeolian rather than fluvial deposits adjacent to Assur. The mineralogy most closely aligns with sources that are situated within 30–50 km of Assur, but on the opposite bank of the Tigris River. This finding suggests that by the early third millennium BC, that is aligned with the Early Dynastic I period as originally indicated by Andrae, the inhabitants of Assur deliberately chose sand from a more distant region, with an appearance that is distinct from the nearby river sand readily available to them found adjacent to the site. We can safely rule out any natural deposition of the temple sand because it is found well above the modern Tigris today and is only found in the temple, demonstrating that it was transported by human activity rather than deposited naturally. This choice may have been linked to the southern Mesopotamian tradition of using pure sand for a temple's foundations, which may typically come from deposits similar to the Injana Formation. The use of sands that are closely comparable in appearance to those of the Injana Formation and can be described as visually mimicking these sands may suggest a deliberate selection process of the materials. Such sands are better sorted, easier to extract from dunes, and potentially more visually pleasing for temple purification.

If it was indeed the sand's appearance that was the crucial factor in its choice, the mineralogical analyses offer an intriguing additional

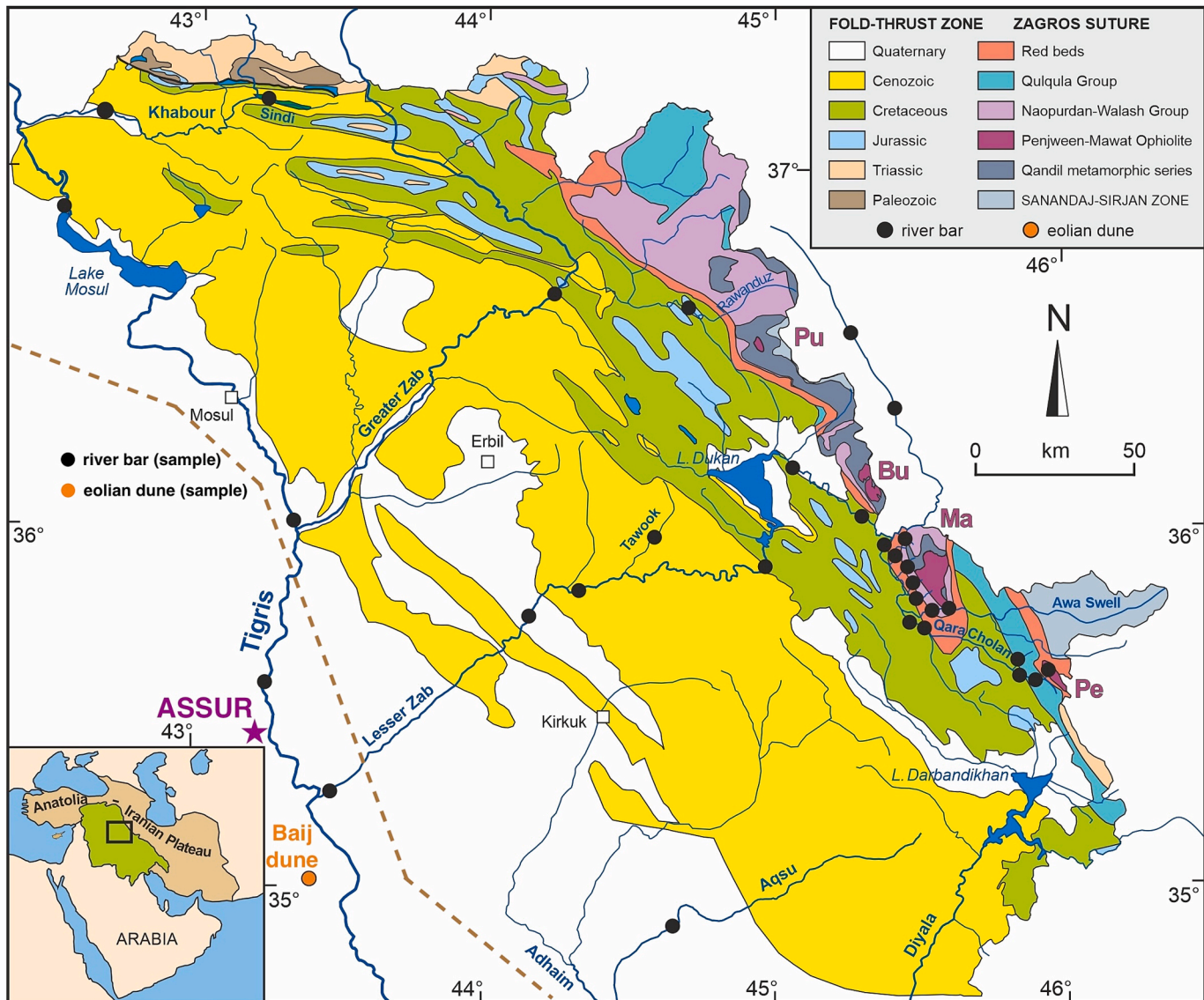


Fig. 10. Geological map of Iraqi Kurdistan showing tectonic domains drained by the Zagros tributaries of the Tigris River and indicating the locations of Assur and the Baij dune field. Black and orange dots indicate the locations of the sand samples discussed in this paper, after [Garzanti et al. \(2016\)](#). The dashed brown line indicates the easternmost border of the Injana formation (based on [Jassim and Buday, 2006, fig. 14.14](#)).

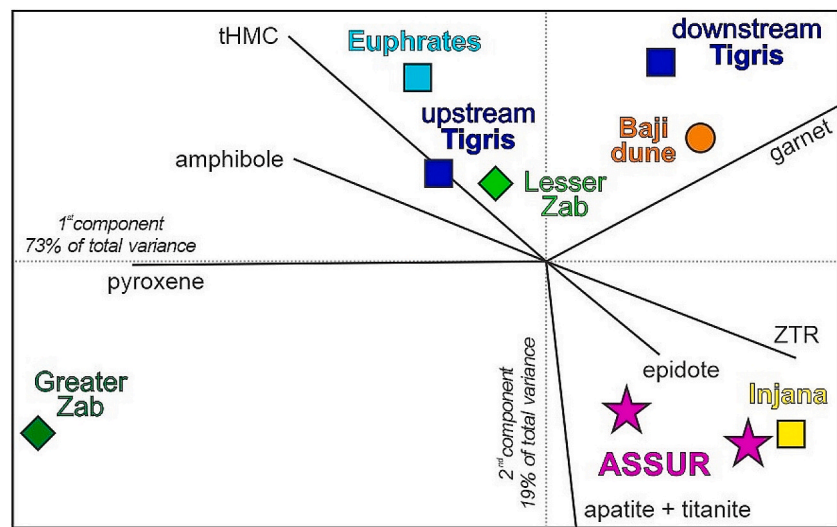


Fig. 11. The biplot highlights the affinity of the Assur sand samples 36 and 37 with sandstones of the Injana Formation and the dissimilarities to all fluvial sands in the region. The compositional biplot (Gabriel, 1971) allows discrimination among multivariate observations (points) while shedding light on the mutual relationships among multiple variables (rays). The length of each ray is proportional to the variance of the corresponding variable; if the angle between two rays is 0° or 180° , then the corresponding variables are perfectly correlated or anticorrelated, respectively.

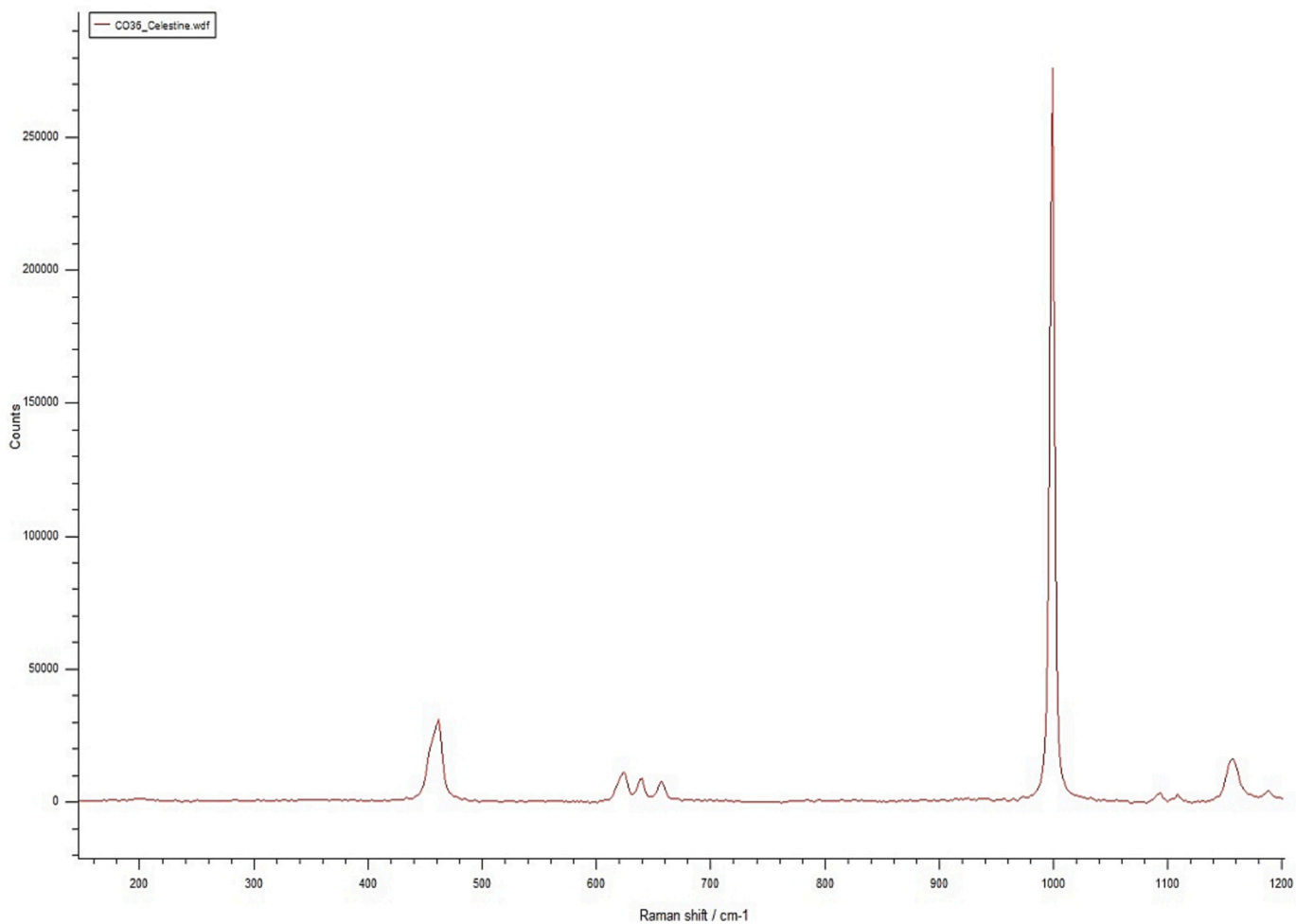


Fig. 12. Raman spectrum of celestite from Assur sand sample 36, indicating reworking of local sulfate crusts. Vibrational modes displayed in the spectrum are compared from literature and own standards of celestite. Counts are arbitrary units of peak intensity, and the position of peaks is expressed in cm^{-1} . The main vibrational peak represents the stretching mode of SO_4^{2-} groups at $\sim 1001 \text{ cm}^{-1}$.

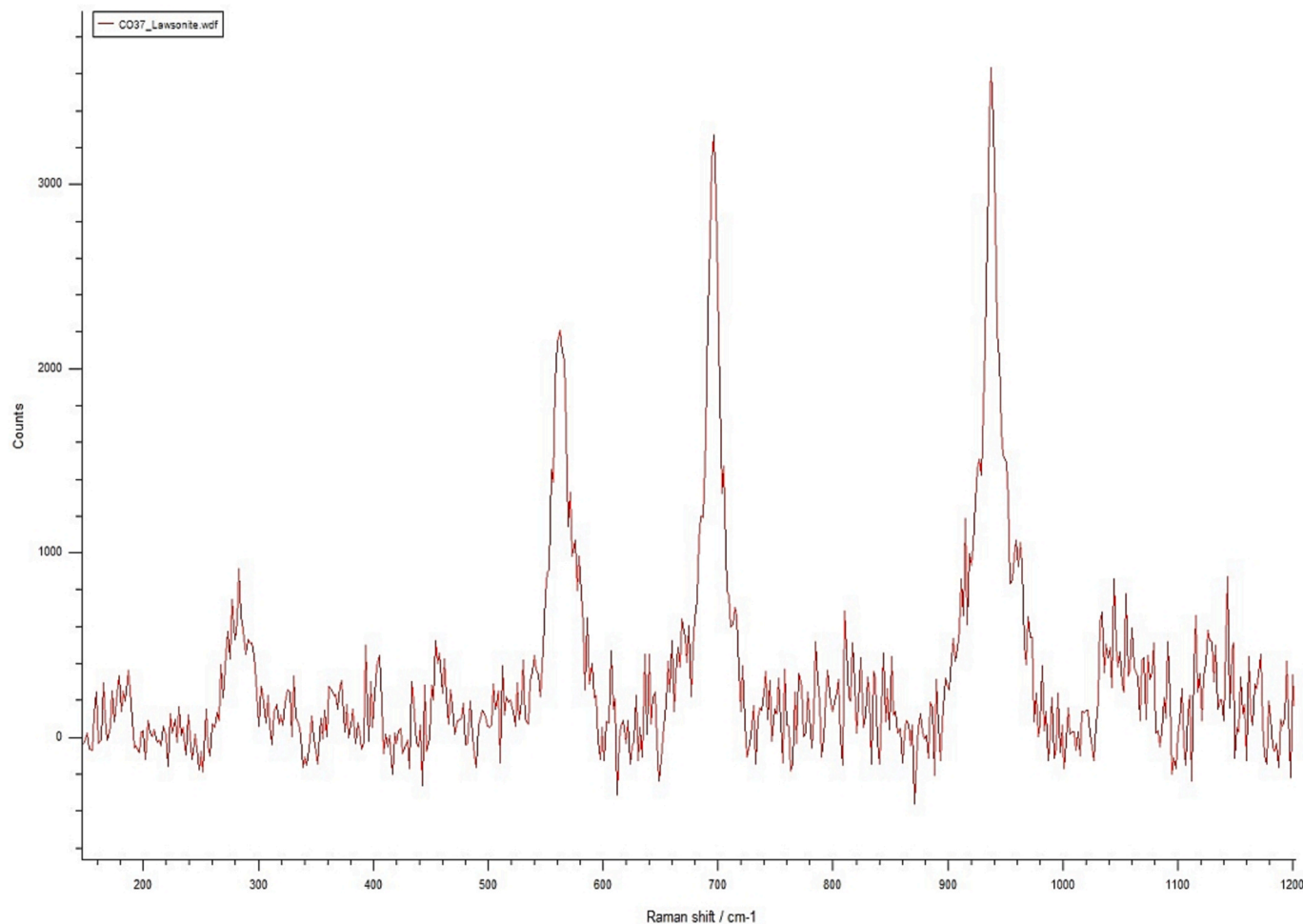


Fig. 13. Raman spectrum of a lawsonite grain from Assur sand sample 37, indicating a provenance from blueschist-facies rocks of the Zagros suture zone. Vibrational modes displayed in the Raman spectrum are compared from literature and own standards of lawsonite. Counts are arbitrary units of peak intensity, and the position of peaks is expressed in cm^{-1} . The main vibrational peaks of lawsonite are located at $\sim 562 \text{ cm}^{-1}$, 697 cm^{-1} , and 940 cm^{-1} .

dimension to the observation that the deposition of sand below the Ishtar Temple suggests knowledge of southern Mesopotamian ritual traditions. This would strengthen the hypothesis that the cult of Ishtar at Assur is linked to that of the goddess Inana in southern Mesopotamia. On the other hand, the sand may have been chosen not for its appearance but for its place of origin. The sand derives from a geographical area whose culture in the third millennium BC was predominantly Hurrian (Wilhelm, 1989: 5-12). This opens up the intriguing possibility that the sand was chosen because it comes from a region that was under the auspices of the Hurrian goddess Shawushka (also known as Shaushka). Like the goddess Ishtar worshipped at nearby Nineveh (modern Mosul) and Arbela (modern Erbil), the Ishtar for whom the temple in Assur was built may have been intimately connected to this eminent Hurrian deity. Of course, the links to southern Mesopotamia and the Hurrian region are not mutually exclusive, and the inhabitants of Assur, situated at a key traffic point between the two areas, may have deliberately sought to combine both traditions when establishing their goddess's sanctuary and cult. As the other temples explored by coring in Assur do not show any sand in their foundations, the Ishtar Temple stands out as a special case that merited specific building practices, likely in order to link the deity to her place of origin, which was not deemed necessary for temples at Assur more generally.

6. Conclusion

This work highlights the benefits of integrating archaeological,

historical, mineralogical, and geoarchaeological data to gain new cultural insights. The results demonstrate that the Ishtar Temple at Assur was established by the Early Dynastic I period, with sands derived from the Zagros region used in its foundation. While sands have been ignored as materials that provide relevant information on the potential origins of key architectural characteristics in Mesopotamian architecture, this paper demonstrates how such materials can be used to identify sources of sand used in architecture and, potentially, in other material culture, and to elucidate cultural connections that may otherwise remain hidden.

CRediT authorship contribution statement

Mark Altawee: Writing – review & editing, Writing – original draft, Methodology, Formal analysis, Data curation, Conceptualization. **Andrea Squitieri:** Writing – review & editing, Writing – original draft, Validation, Methodology, Formal analysis, Data curation, Conceptualization. **Eileen Eckmeier:** Writing – review & editing, Writing – original draft, Methodology, Data curation, Conceptualization. **Eduardo Garzanti:** Writing – review & editing, Writing – original draft, Methodology, Formal analysis, Data curation. **Karen Radner:** Writing – review & editing, Writing – original draft, Methodology, Funding acquisition, Data curation, Conceptualization.

Declaration of competing interest

The authors declare that they have no known competing financial

interests or personal relationships that could have appeared to influence the work reported in this paper.

Acknowledgments

This research was conducted within the framework of the renewed excavations at Assur, funded by the Gottfried Wilhelm Leibniz Award of the German Research Foundation (DFG) awarded to Karen Radner in 2022. The authors are grateful to the authorities of the State Board of Antiquities and Heritage of Iraq (SBAH) for their trust and continued support, and to the members of the SBAH Salahaddin Directorate for their invaluable logistical assistance and cooperation.

Appendix A. Supplementary data

Supplementary data to this article can be found online at <https://doi.org/10.1016/j.jasrep.2026.105574>.

Data availability

The data are available in the article and supplementary data

References

Altaweel, M., 2025. The 2024 geoarchaeological coring at Assur. In: Radner, K., Squitieri, A. (Eds.), *Assur 2024: Continuing the Excavations in the New Town and Other Research across the Site (exploring Assur 2)*. PeWe Verlag, Gladbeck, pp. 26–33.

Ambos, C., 2004. Mesopotamische Baurituale aus dem 1. Jahrtausend v. Chr. ISLET, Dresden.

Andrae, W., 1922. Der archaische Ishtar-Tempel in Assur (Wissenschaftliche Veröffentlichungen der Deutschen Orient-Gesellschaft 39). Leipzig, J.C. Hinrichs.

Andrae, W., 1935. Die jüngeren Ishtar-Tempel in Assur (Wissenschaftliche Veröffentlichungen der Deutschen Orient-Gesellschaft 58). Leipzig, J.C. Hinrichs.

Andrae, W., 1938. Das wiedererstandene Assur. Leipzig, J.C. Hinrichs.

Andò, S., Garzanti, E., 2014. Raman spectroscopy in heavy-mineral studies, in: Scott, R. A., Smyth, H.R., Morton, A.C., Richardson, N. (Eds.), *Sediment Provenance Studies in Hydrocarbon Exploration and Production*. Geological Society London, Special Publication 386, pp. 395–412.

Angiolini, L., Balini, M., Garzanti, E., Nicora, A., Tintori, A., 2003. Gondwanan deglaciation and opening of neotethys: the Al Khlata and Saiwan formations of interior Oman. *Palaeogeogr. Palaeoclimatol. Palaeoecol.* 196 (1–2), 99–123.

Averbeck, R.E., 2010. Temple building among the Sumerians and Akkadians (third millennium). In: Boda, M.J., Novotny, J. (Eds.), *From the Foundations to the Crenellations: Essays on Temple Building in the Ancient Near East and Hebrew Bible*. Ugarit-Verlag, Münster, pp. 3–34.

Bär, J., 2003a. Die älteren Ishtar-Tempel in Assur (Wissenschaftliche Veröffentlichungen der Deutschen Orient-Gesellschaft 105). Harrassowitz, Wiesbaden.

Bär, J., 2003b. Sumerians, Gutians and Hurrians at Ashur? A re-examination of Ishtar Temples G and F. *Iraq* 65, 143–160.

Beuger, C. 2013. Die Keramik der älteren Ishtar-Tempel in Assur von der zweiten Hälfte des 3. Jahrtausends bis zur Mitte des 2. Jahrtausends v. Chr. (Wissenschaftliche Veröffentlichungen der Deutschen Orient-Gesellschaft 138). Harrassowitz, Wiesbaden.

Brems, D., Pauwels, J., Blomme, A., Scott, R.B., Degryse, P., 2015. Geochemical heterogeneity of sand deposits and its implications for the provenance determination of Roman glass. *Star* 1 (2), 115–124. <https://doi.org/10.1080/20548923.2016.1184915>.

Briant, R.M., Jotheri, J., Al-Ameri, I., Ahmed, A., Bateman, M.D., Engels, S., Garzanti, E., Nymark, A., Reynolds, T.E., 2024. Disentangling late Quaternary fluvial and climatic drivers of palaeohydrological change in the Najaf Sea basin. *Western Iraq. Earth Surf. Process. Landf.* 49 (4), 1451–1467.

Bronk Ramsey, C., 2021. OxCal v.4.4.4 [software]. URL: <https://c14.arch.ox.ac.uk/oxcal.html>.

Ellis, R.S., 1968. *Foundations Deposits in Mesopotamia*. Yale University Press, New Haven / London.

Folk, R., 1981. *Petrology of Sedimentary Rocks*, 2nd ed. Hemphill Publishing Company, Austin.

Gabriel, K.R., 1971. The biplot graphic display of matrices with application to principal component analysis. *Biometrika* 58 (3), 453–467.

Garzanti, E., 2017. The maturity myth in sedimentology and provenance analysis. *J. Sediment. Res.* 87, 353–365. <https://doi.org/10.2110/jsr.2017.17>.

Garzanti, E., Andò, S., 2019. Heavy minerals for junior woodchucks. *Minerals* 9 (3), 148. <https://doi.org/10.3390/min9030148>.

Garzanti, E., Al-Juboury, A.I., Zoleikhaei, Y., Vermeesch, P., Jotheri, J., Akkoca, D.B., Obaid, A.K., Allen, M.B., Andò, S., Limonta, M., Padoan, M., 2016. The Euphrates-Tigris-Karun river system: provenance, recycling and dispersal of quartz-poor foreland-basin sediments in arid climate. *Earth Sci. Rev.* 162, 107–128.

Haas, V., 1979. Remarks on the Hurrian Istar-Šawuška of Nineveh in the second millennium BC. *Sumer* 35, 401.

Kettanah, Y.A., Abdulrahman, A.S., 2022. Petrography and geochemistry of sandstones from the Injana Formation, Hemrin South Mountain, Northern Iraq: implications for provenance, weathering and tectonic setting. *Geol. J.* 57 (5), 2007–2023.

Jassim, S.Z., Buday, T., 2006. Latest Eocene-Recent Megasequence AP11. In: Jassim, S.Z., Goff, J.C. (Eds.), *Geology of Iraq*. Dolin, Prague and Moravian Museum, Brno, pp. 228–253.

Leacroft, H., Leacroft, R., 1974. *The buildings of ancient Mesopotamia*. Brockhampton Press, Reading.

MacGinnis, J., 2014. *A city from the dawn of history: Erbil in the cuneiform sources*. Oxbow, Oxford.

Meinholt, W., 2009. *Istar in Assur: Untersuchung eines Lokalkultes von ca. Chr. Ugarit-Verlag*, Münster, 2500 bis 614 v.

Miglus, P., 2003. Neue Forschungen in Assur. In: Marzahn, J., Salje, B. (Eds.), *Wiedererstehendes Assur: 100 Jahre Deutsche Ausgrabungen in Assyrien*. Philipp von Zabern, Mainz, pp. 183–189.

Radner, K., Squitieri, A. (Eds.), 2024. *Assur 2023: Excavations and Other Research in the New Town (exploring Assur 1)*. PeWe-Verlag, Gladbeck.

Radner, K., Squitieri, A. (Eds.), 2025. *Assur 2024: Continuing the Excavations in the New Town and Other Research across the Site (exploring Assur 2)*. PeWe-Verlag, Gladbeck.

Reimer, P.J., Austin, W.E.N., Bard, E., et al., 2020. The IntCal20 northern hemisphere radiocarbon age calibration curve (0–55 cal kBP). *Radiocarbon* 62 (4), 725–757. <https://doi.org/10.1017/RDC.2020.41>.

Schmitt, A., 2012. Die jüngeren Istar-Tempel und der Nabû-Tempel in Assur (Wissenschaftliche Veröffentlichungen der Deutschen Orient-Gesellschaft 137). Harrassowitz, Wiesbaden.

Schwemer, D., 2001. *Die Wettergottgestalten Mesopotamiens und Nordsyriens im Zeitalter der Keilschriftkulturen*. Harrassowitz, Wiesbaden.

Secco, M., Previato, C., Addis, A., Zago, G., Kamsteeg, A., Dilaria, S., Canovaro, C., Artioli, G., Bonetto, J., 2019. Mineralogical clustering of the structural mortars from the Sarno Baths, Pompeii: a tool to interpret construction techniques and relative chronologies. *J. Cult. Herit.* 40, 265–273. <https://doi.org/10.1016/j.culher.2019.04.016>.

Seidl, U., 2005. The Urartian Istar-Šawuška. In: Çilingiroğlu, A., Darbyshire, G. (Eds.), *Anatolian Iron Ages 5* (British Institute of Archaeology at Ankara Monograph 31). British Institute of Archaeology at Ankara, Ankara, pp. 167–173.

Sissakian, V., Al-Ansari, N., Knutsson, S., 2014. Origin of some transversal linear features of NE-SW trend in Iraq, and their geological characters. *Nat. Sci.* 6, 996–1011. <https://doi.org/10.4236/ns.2014.612091>.

Talbot, C.J., 2019. High-pressure/low-temperature blueschists in the Zagros Mountains. In: Farzipour Saein, A. (Ed.), *Developments in Structural Geology and Tectonics*, 3. Elsevier, Amsterdam, pp. 75–82.

Wegner, I., 1981. *Istar-Šawuška: Gestalt und Kult der Istar-Šawuška in Kleinasien*. Kevelaer/Neukirchner Verlag, Neukirchen-Vluyn, Butzon & Bercker.

Werner, P., 2009. Der Sin-Samas-Tempel in Assur (Wissenschaftliche Veröffentlichungen der Deutschen Orient-Gesellschaft 122). Harrassowitz, Wiesbaden.

Werner, P., 2016. Der Anu-Adad-Tempel in Assur (Wissenschaftliche Veröffentlichungen der Deutschen Orient-Gesellschaft 145). Harrassowitz, Wiesbaden.

Wilhelm, G., 1989. *The Hurrians*. Aris & Phillips, Warminster.

WRB, 2022. *World Reference Base for Soil Resources. International soil classification system for naming soils and creating legends for soil maps*, 4th edition. International Union of Soil Sciences (IUSS), Vienna, Austria.